Polymer Bulletin (2020) 77:3017–3031
https://doi.org/10.1007/s00289-019-02888-8

ORIGINAL PAPER

Multicomponent polyurethane–carbon black composite as piezoresistive sensor

Eliraldrin Amorin Sousa[1] · Thalita Hellen Castro Lima[1] · Elen Poliani Silva Arlindo[1] · Alex Otávio Sanches[2] · Walter Katsumi Sakamoto[2] · Gilberto de Campos Fuzari-Junior[1]

Received: 9 February 2019 / Revised: 2 June 2019 / Accepted: 24 July 2019 / Published online: 31 July 2019

Abstract

Composite of carbon black (CB) dispersed into a multicomponent polyurethane matrix combines the good mechanical properties of the polymer, such as elasticity, with the electrical property of the conducting particles. Electrical current–voltage ($I \times V$) analysis found the percolation threshold through the sample surface to be between 0.6 and 0.8 vol%. Below the percolation threshold concentration (p_c), the effect of the Coulomb potential is accentuated on the CB dispersion, while in the region over p_c, the London–van der Waals potential is important. The repeatability in the piezoresistive behavior was observed under the application of several loading cycles. The gauge factors obtained were 4.9 and 2.0 for samples with 0.8 and 1.0 vol% of CB, respectively. The results indicate that the material can be used as a piezoresistive sensor.

Keywords Polyurethane · Carbon black · Piezoresistance

Introduction

Currently, the need for more efficient and effective control of the structural integrity of materials in any area of application is growing. The demands of society as a whole for better products, greater comfort, and safety have motivated research in the so-called structural health monitoring area.

The structural evaluation technique requires a good performance sensor, which has contributed to the development of research in the area of sensors. The use of sensors covers a wide range of applications such as textile, automotive, medical,

✉ Eliraldrin Amorin Sousa
eliraldrin@gmail.com

[1] Instituto de Ciências Exatas e da Terra, Campus Universitário do Araguaia, Universidade Federal de Mato Grosso, Barra Do Garças 78600-000, Mato Grosso, Brazil

[2] Departamento de Física e Química, Faculdade de Engenharia de Ilha Solteira, Universidade Estadual Paulista, Ilha Solteira 15385-000, São Paulo, Brazil

aerospace, and civil engineering, among others [1–6]. The nondestructive, accurate evaluation of the integrity of a building in a short time contributes to the reduction of maintenance costs and avoids tragedies.

In the development of sensors, metallic, ceramic, and polymeric materials were studied as sensors in several applications. Each application requires a certain type of sensor, and each specific application requires an appropriate material for the construction of the sensor. However, considering the mechanical and electrical properties as well as the problem of flexibility, weight, and impact resistance, one-phase materials may have some restriction. In this context, composite materials, which combine properties of one-phase materials to improve their performance as a sensor, appear as alternative materials to be studied.

An interesting sensor for evaluating structures is the so-called piezoresistor, which changes its electrical resistivity when a mechanical stimulus is applied to it. The study of the piezoresistive effect in polymer matrix composites has attracted the attention of many researchers because the sensor material becomes a self-detector material for stress or strain and shows high sensitivity [7–9]. Thus, certain advantages appear in piezoresistive materials, such as low cost, useful lifetime, and higher volume detection, because all structures have detection capabilities, and there is no degradation of mechanical properties [10, 11].

High sensitivity in the deformation detection of the composite material is very important for structural deformation monitoring in many areas such as in the civil engineering of structures, transportation systems, and equipment [11, 12]. In all these areas, monitoring structural integrity, lifetime, and performance are fundamental for safety and economic efficiency.

During the deformation of the structure under analysis, the sensor material is also deformed. This changes its electrical resistance, which can be observed in an appropriate measuring system [13]. Furthermore, the piezoresistive effect is used in several applications, including accelerometers, sensors for pressure, tactile sensitivity, and flux, as well as chemical and biological sensors, which require compatible materials (e.g., artificial skin, prostheses) [14–18]. Wu et al. proposed a simple, cost-efficient, and large-area compliant strategy for fabricating a highly sensitive strain sensor by coating polyurethane (PU) yarn with a conductive polymer composite layer consisting of carbon black (CB) and natural rubber. This composite yarn strain sensor exhibited high sensitivity with a gauge factor of 39 and a detection limit of 0.1% strain [19]. Li et al. studied polyurethane composites with conducting CB. The percolation threshold is achieved at the CB concentration of 20 wt%. Polyurethane composites with CB have displayed the combination of both shape memory properties and electric conductivity [20]. Polyurethane is a class of polymer containing urethane linkages. In this work, the urethane will be a reaction product between an isocyanate group and a hydroxyl group [21]. Other works have investigated the adsorption behavior of steam and its influence on the gas sensitivity of water-based polyurethane composites, and conductive CB conductors were studied regarding the relationship between the vapor adsorption behavior and the electrical responsiveness of the composites [22, 23].

In the present work, flexible films of multicomponent polyurethane (MCPU) and CB composite were obtained, and the piezoresistive effects were studied to propose

this material as a sensor for a nondestructive analysis technique. The polymer matrix, commercially named UltraFlex PU, is an elastic polymer-based sealant used in civil constructions for joint connections, windows, and general seals. The product cures upon contact with room humidity, forming a high-strength elastomer.

In the MCPU/CB composite, the relation between electrical and mechanical properties in polyurethane/carbon black had a tendency to form a conductor path in the insulator matrix. When a critical concentration value is reached, it defines the percolation threshold. From this concentration value, the electrical conductivity of the composite material increased significantly due to the formation of at least one conductor path in the insulator matrix [24]. The piezoresistivity observed on this composite sensor can be attributed mainly to the tunneling effect in adjacent particles and the contact loss between the inclusion materials with the deformation variation [25].

The UltraFlex polymer matrix is because it is already used in civil construction on structures that eventually could be evaluated, because it is more appropriate to have a sensor material surface installed into the structure allowing greater detection capacity.

Materials and methods

Materials

The multicomponent polyurethane UltraFlex PU for construction of ITW POLYMERS® with 1.32 g/cm^3 density was used in a paste form. The MCPU contained the following: polyurethane (predominantly), titanium dioxide (0–4%), carbon black (0.2–1%), and vinyltrimethoxysilane (1–2%). CB particles with 50 nm diameter, 1000 m^2/g of area, density equal to 2.0 g/cm^3, and a 99% degree of purity were purchased from Cabot.

MCPU/CB composite preparation

The composite films were prepared by dispersing CB particles into isopropyl alcohol using an ultrasound for 60 min. The polymer MCPU was also dispersed into the isopropyl alcohol (Sigma-Aldrich®) for 30 min. After that, both solutions were mixed and stirred for 180 min. The final solution was then poured onto plastic film (Parafilm®) for evaporation of the solvent at room temperature. The film had a medium thickness of 550 μm.

Sample characterizations

Figure 1 shows how the system was used for the piezoresistive tests of the MCPU/CB composite. The sample was under cyclic axial stress, with a velocity of 12.5 mm/min. The mechanical deformation (ε) was calculated by the claw displacement and normalized by the useful length of the sample. Both stress–strain and piezoresistive

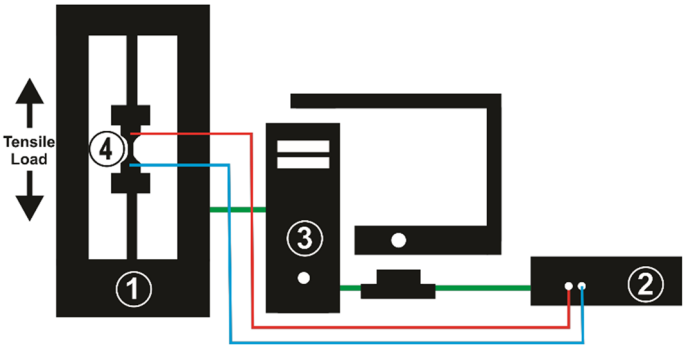

Fig. 1 Image of equipment used in the piezoresistive test: (1) universal test machine WDW-30E, (2) Keithley Mod. 2611, (3) computer for data record, and (4) sample

measurements were taken at room temperature using 12.5 mm/min deformation velocity, with a load cell of 600 N in the Universal Test Equipment Model WDW-30E. The sample shape is according to ASTMD1708-10 standards. The electrical resistance was measured in situ during the stress test using the Keithley model 2611 as a current source. The piezoresistive test was performed in composite films with 0.8 and 1.0 vol% of CB. This filler content range was used because for composite samples with lower CB content, the high value of electrical resistance did not allow that measurement, and for volume fractions higher than 1.0 vol% of CB, the piezoresistive analysis became difficult because the sample displayed poor mechanical resistance. The piezoresistive sensibility of the composite films was quantified by the calibration factor or gauge factor (GF) measured in the elastic regions of the samples, which were $\varepsilon \leq 25\%$ and $\varepsilon \leq 22.5\%$, for samples with 0.8 and 1.0 vol%, respectively.

Two connectors were fixed in metal (aluminum) tape and used as an electrode. The metal tape was involved with an insulator tape between the stress–strain test machine. The cables were separated by approximately 30 mm. In the piezoresistance study, the values of the deformation of the samples with 0.8 vol% and 1.0 vol% of CB were close to 25 and 22.5%, respectively.

SEM images were performed on a Zeiss microscope, model Evo LS-15. The samples were previously covered with a layer of gold, deposited by sputtering, which was previously fixed in support of samples using a conductive adhesive tape.

Results and discussion

Electrical conductivity analysis

The electrical conductivity of the MCPU/CB composite can be changed by adding conductor particles into the polymer matrix, which is an insulator. For insignificant amounts of conductor particles dispersed into the polymer matrix, the electrical conductivity increases in comparison with the conductivity of the pure polymer.

However, to reach a significant conductivity level, the particles must be distributed closely to each other, which provides a continuous conductor path through the polymer matrix, i.e., the percolation threshold must be established [26]. Figure 2 shows the conductivity behavior in the composite sample for different volume fractions of the inclusion conductor particles. A significant increase in the conductivity can be observed when the volume fraction of CB reaches 0.8 vol%; beyond 1.0 vol%, there is no significant change in the conductivity. According to the percolation theory, the conductivity of the composite sample near the percolation threshold follows the power law given by the following equation:

$$\sigma \propto \left[p_c - p\right]^{-s} \tag{1}$$

where p_c is the percolation threshold, p is the filler content, and s is a critical exponent, in the range of p lower than p_c. For p higher than p_c, the power law related to the percolation threshold is

$$\sigma \propto \left(p - p_c\right)^{t} \tag{2}$$

with t as the critical exponent.

The insets in Fig. 2 show the fitting obtained, varying by a small quantity of the values of p close to the p_c region. The critical exponents obtained were $s = 1.55$ and $t = 2.22$. It was verified that in the region $(p_c - p)$, below the percolation threshold, the plot log σ × log $(p_c - p)$ shows a marked dispersion away from the power law (Eq. 1), which is reflected in clear distortion presented by the critical exponent. Such occurrence may be related to the local variation in concentration and/or shape and orientation of the filler phase as well as effects of synergistic and electrostatic interactions [27, 28], which reflect in an irregular behavior of the conductivity pattern dominated by tunneling processes. On the other hand, for regions above the

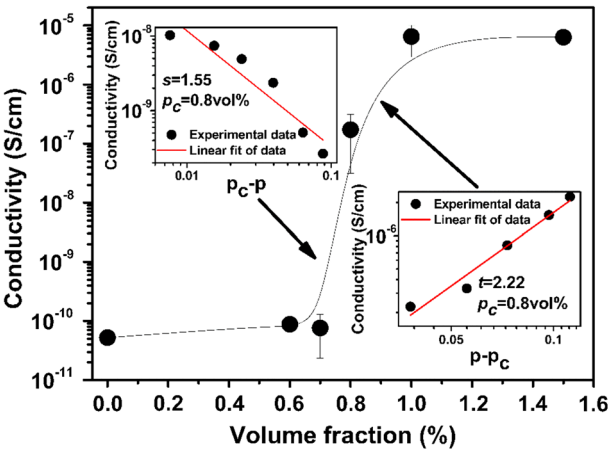

Fig. 2 Electrical conductivity of MCPU/CB measured through the surface of the sample

percolation threshold, with the formation of a continuous physical percolation path, a pattern closer to the classical percolation is observed, which can be observed in the value of the critical exponent $t = 2.22$, indicating the formation of a three-dimensional conducting network. The small deviation found for the critical exponent for this region may be related to the existence of tunneling processes as discussed by Vionnot-Menot et al. [29].

It is worth mentioning that elastomeric matrices filled with CB typically require large filler concentrations (10–20 wt%) [30, 31]. Flexible nanocomposite films derived from castor-oil polyurethane (PUR) and CB nanoparticles were prepared by casting. The PUR/CB nanocomposites exhibited a percolation threshold ($p_c = 5.7$ vol%) [32]. In our work, the percolation threshold is around 1 wt%, close to the value found in the composites of PU/CNT (carbon nanotubes) [33, 34].

Morphological analysis

Scanning electron microscopy (SEM) shows the morphology of pure MCPU and MCPU/CB composites, with the volume fraction of CB varying in the range of 0.6, 0.8, and 1.0 vol%, as shown in Fig. 2.

Based on the electrical conductivity results, it is expected that the interconnective structure of the CB fillers will form along the MCPU polymer matrix. When the CB content is lower than the percolation threshold, the loads exist in the form of isolated aggregates (Fig. 3b), which is why the conductivity is not measurable [35]. For the sample MCPU/CB 0.8 (Fig. 3c), paths form for electric conduction along the

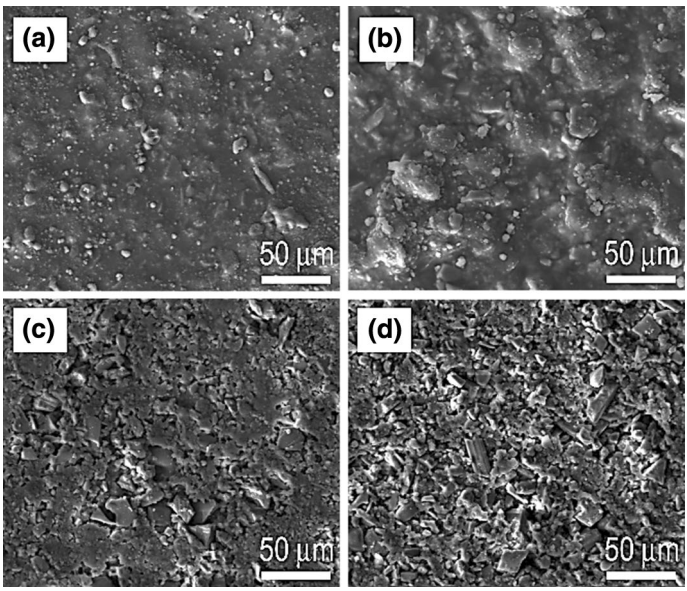

Fig. 3 SEM images of MCPU/CB films with **a** 0.0 vol%, **b** 0.6 vol%, **c** 0.8 vol%, and **d** 1.0 vol% of CB

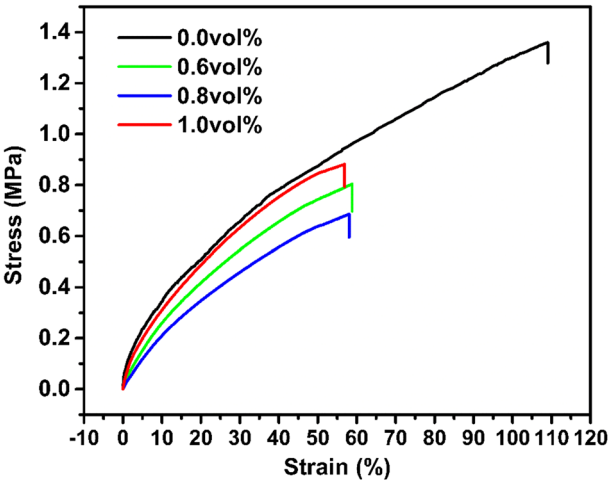

Fig. 4 Stress–strain test

Table 1 Results of stress–strain tests for MCPU/CB composite films with different volume fractions of CB

CB (vol%)	Elongation at break (%)	Tensile strength at break (MPa)
0.0	109 ± 13	1.35 ± 0.04
0.6	59 ± 8	0.80 ± 0.03
0.8	57 ± 4	0.69 ± 0.05
1.0	56 ± 7	0.89 ± 0.02

material and these paths are maximized, increasing the CB content for the concentration of 1.0 vol% (Fig. 3d).

Li et al. reported two possible reasons for the appearance of large aggregates of CB in the polyurethane matrix. One is the relatively low wettability between CB and polar polymers, such as the polyurethane used in this study. The other reason is due to sample preparation. Unlike melt extrusion, the casting method has lower shear strength [20, 36].

Stress–strain tests

The stress–strain tests for MCPU/CB composite films with different volume fractions of CB are shown in Fig. 4.

Elongation at break and tensile strength at break values of the samples are shown in Table 1.

The stress–strain curves reflect a decrease in the maximum deformation with increasing CB concentration. The agglomerates of CB present in these composites caused cracks to initiate and propagate easily. Such generated cracks usually reduce

the strength of the composite. Samples with higher amounts of CB, mainly MCPU/CB 0.8% and MCPU/CB 1.0%, show a reduction in elongation at rupture, probably due to problems related to the increase in MCPU/CB interfaces, immiscible phases in which (physical) interactions are probably fragile [37]. In other works, the mechanical properties presented similar behavior in relation to the elastic regime. In this study, conductive cellulose nanofibril/AgNWs (CA)-coated PU (CA@PU) sponge was fabricated using a simple dip-coating technique, and in the work of Christ and co-workers, the elastic region was around 20% strain [38, 39]. Comparing the properties of these materials with the composite obtained in this work, it is suggested that the MCPU/CB composite has potential application for piezoresistive sensors.

Piezoresistance study

The piezoresistance response of the composite film was analyzed in situ while the films were mechanically stretched across an elastic region. Figure 5 shows the electrical resistance variation in the elastic regime of the samples with 0.8 and 1.0 volume fractions of CB while 10 loading–unloading test cycles were carried out. For each cycle, the film deformation increased linearly with the applied stress. Similar slope was observed during the unloading until it reached zero stress. In addition, a temporal delay in the response of the electrical resistance to the deformation was observed, which can be attributed to the internal viscoelasticity of the polymer, related to the time of organization of the polymer chains against the applied mechanical strain. Thus, the initial increase in the resistivity at concentrations above the percolation threshold occurred due to the breakdown of the physical percolation network formed by the CB, resulting in smaller aggregates and a significant reduction of the conduction paths. In the case of concentrations

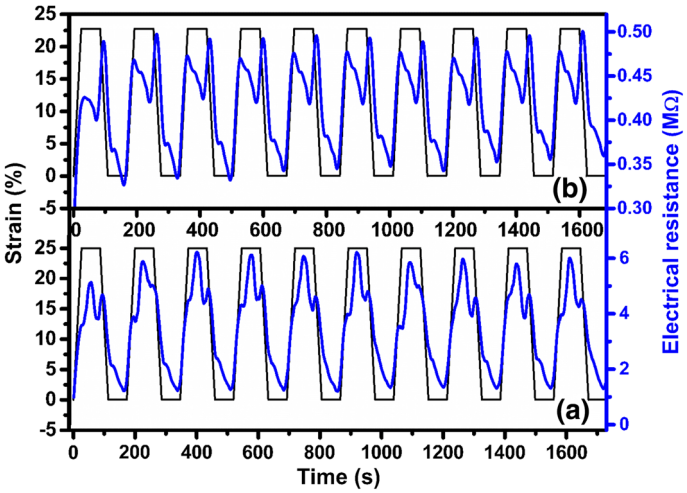

Fig. 5 Loading–unloading cycles applied to MCPU/CB films: **a** 0.8 vol% and **b** 1.0 vol% of CB

below the percolation threshold, the reduction in resistivity was mainly due to the breakdown of the percolated electric net resulting from the increased distance of the aggregated CB, making tunneling processes difficult. Therefore, in both cases, as the mechanical stress was held constant, the CB aggregates began to rotate and align the polymer chains together in the direction of the uniaxial stress, resulting in the observed decrease in resistivity in that period in both samples. As this alignment reached its maximum and the mechanical tension was maintained, the CB aggregates then aligned again and increased their distance, resulting in a second increase in the electrical resistance observed at the end of the period of application of the constant mechanical stress in both cases presented. When the mechanical stress was removed from the samples, a sudden drop in the resistance was observed that can be attributed to the reconstruction of both physical and electrical percolated paths. However, as can be seen, due to the viscoelasticity of the polymer, this reduction of the resistance to its stabilization level was not instantaneous with the removal of the mechanical stress. It was observed that the maximum strength obtained during the tests for different CB fractions occurred at different times during the application of constant mechanical stress, which was due to the fact that the process of maximum alignment of CB particles occurs in late periods for concentrations below the percolation threshold.

Figure 6 shows the piezoresistance behavior during four cycles for samples with 0.8 and 1.0 vol% of CB. The electrical resistance does not return to its original value after the first cycle. As the inclusion particles' volume fraction increases, this effect becomes more evident. This fact can be attributed to some irreversible damage that occurred during the first loading–unloading cycle [40]. This effect has been observed by many authors working with elastomer/CB composites and can be explained as a permanent change in the conductive network

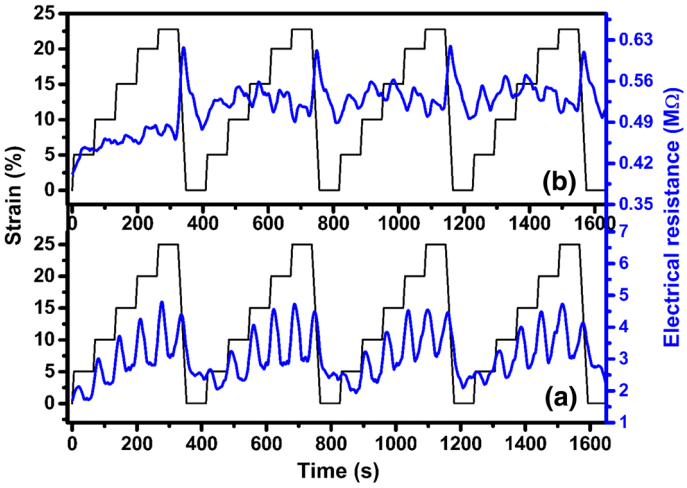

Fig. 6 Cycles with gradual increases of mechanical deformation of the composite at **a** 0.8 vol% and **b** 1.0 vol% of CB

as well as in the microstructure of the polymer matrix due to the deformation [39–47].

Figure 7 shows the piezoresistive behavior of 0.8 and 1.0 vol% of inclusions in MCPU/CB composites under continuous cycles of deformation. For each cycle, the loading nears the yield strength. When the load is removed, the electrical resistance is recovered and has a tendency to follow the applied stress.

The results in Fig. 7 were used to analyze the piezoresistive response of the samples, verifying the repeatability and stability of these sensors and the essential parameters for use as a sensor under a regime of various mechanical deformations. In this work, 30 cycles that displayed acceptable behavior were performed.

Measurements in the fifth cycle, shown in Fig. 5, were utilized for obtaining the gauge factor, and Fig. 8 specifies the relative electrical resistance as a function of the applied deformation to the composite film, with 0.8 and 1.0 vol% of the CB.

Linear regression was used for the point's adjustment, which was also used by Ku-Herrera and co-workers [43, 44]. The values of the gauge factor (GF) for the MCPU/CB samples are listed in Table 2 in comparison with some values reported in the literature.

The GF values obtained for the MCPU/CB composites are close to those presented by metal sheet deformation sensors and much smaller than semiconductor-based sensors. However, the main disadvantages of these semiconductor and metallic piezoresistors are their brittleness and rigidity, and the production of semiconductor materials is much more expensive in comparison with that of the polymer-based composite [50]. An important point of the MCPU/CB is that its matrix is a sealant base and that it can be used in civil construction or other applications that require a sensor adhered to the structure to be monitored.

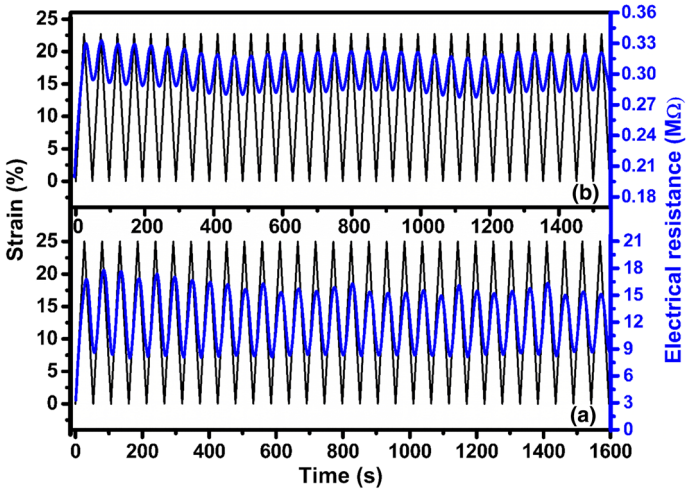

Fig. 7 Cyclic loading of **a** 0.8 vol% and **b** 1.0 vol% of CB

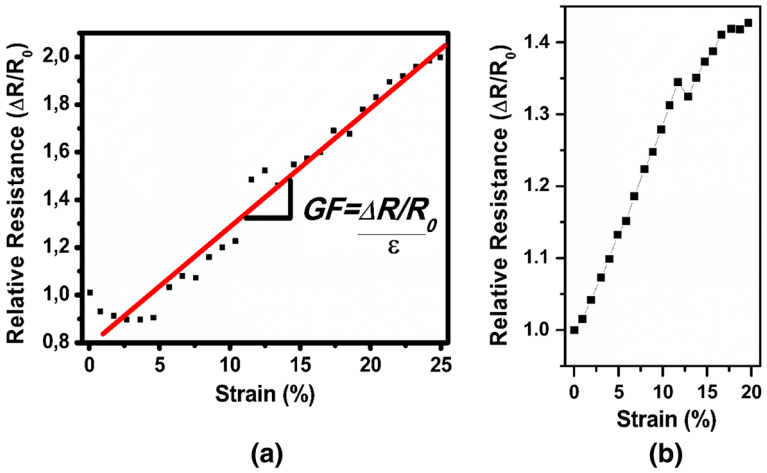

Fig. 8 Piezoresistive curve for MCPU/CB samples: **a** example of the linear approach used to calculate the gauge factor (GF) 0.8 vol% and **b** 1.0 vol% of CB

Table 2 Values of GF for some main material used in the deformation sensor manufacture and GF for the MCPU/CB composite

Material of sensor	GF
Multilayer carbon nanotube and vinyl ether	2.3–2.6 [47]
Crystalline silicon	50–150 [48]
Metal sheets	2–5 [49]
MCPU/CB 0.8 vol%	4.9 ± 0.2
MCPU/CB 1.0 vol%	2.0 ± 0.1

Table 2 shows that the GF value of the sample with 1.0 vol% of CB is lower than that of the sample with 0.8 vol%. The decreasing piezoresistive sensibility with an increased amount of CB was reported in some works [51–53]. The electrical resistance of the composite film depends on the CB content, among many other factors. For a high concentration, there is more contact between the CB particles, which increase the conductor path's density and consequently the electrical conductivity of the sample. However, for the piezoresistance, the relation between sensibility and volume fraction does not follow the same law.

As considered by other researchers, the dominant parameters of the piezoresistive response seem to be the percolate network geometry, the structure of CB particles, and the relative contribution of tunneling resistance to the total electrical resistance [52, 54, 55]. Both the CB network contribution and the capability to enhance the tunneling resistance were optimized for low CB concentrations because better particle dispersion was reached [52]. However, very low CB concentration means low electrical conductance, which makes it difficult to measure ΔR. Although the CB concentration that made the sample more sensitive occurred slightly above the percolation threshold, Hu and collaborators stated that the relation between piezoresistive sensibility and the electrical current requires CB content far above the percolation threshold [52, 56].

Conclusions

MCPU/CB composite films were obtained with different electrical conductivities according to their amounts of carbon black inclusion particles. They were analyzed by stress–strain tests, and it was verified that the material only interferes with the structure to be monitored to a small degree. Therefore, it can be used as a sensor. Piezoresistive analysis under various loading–unloading cycles indicates that the material has stability, and the electrical resistance response is repeatable. The unrecovered electrical resistance is related to the permanent change in the conducting network and microstructure of the polymer. A temporal delay in the electrical resistance response in relation to the deformation was observed in the composites and attributed to the internal viscoelasticity of the polymer. The gauge factor of the composite is similar to the one shown by a metallic sheet sensor.

Acknowledgements Thanks are due to Coordination for the Improvement of Higher Level or Education Personnel (CAPES) for financial support and to the Mato Grosso Research Foundation (FAPEMAT) for providing equipment to the laboratory and allowing for analysis.

References

1. Capineri L (2014) Resistive sensors with smart textiles for wearable technology: from fabrication process to integration with electronics. Procedia Eng 87:724–727. https://doi.org/10.1016/j.proeng.2014.11.748
2. Abdelhamid S, Hassanein HS, Takahara G (2014) Vehicle as a mobile sensor. Procedia Comput Sci 34:286–295. https://doi.org/10.1016/j.procs.2014.07.025
3. Ciuti G, Ricotti L, Menciassi A, Dario P (2015) MEMS sensor technologies for human centred applications in healthcare, physical activities, safety and environmental sensing: a review on research activities in Italy. Sensors 15:6441–6468. https://doi.org/10.3390/s150306441
4. Person MR, Eaton MJ, Pullin R, Featherston CA, Holford KM (2012) energy harvesting for aerospace structural health monitoring systems. J Phys Conf Ser 382:012025. https://doi.org/10.1088/1742-6596/382/1/012025
5. Lyndon M, Robinson D, Taylor SE, Amato G, Brien EJO, Uddin N (2017) Improved axle detection for bridge weigh-in-motion systems using fiber optic sensors. J Civil Struct Health Monit 7:325–332. https://doi.org/10.1007/s13349-017-0229-4
6. Xie J, Long H, Miao M (2016) High sensitivity knitted fabric strain sensors. Smart Mater Struct 25:105008. https://doi.org/10.1088/0964-1726/25/10/105008
7. Dai H, Thostenson ET, Schumacher T (2015) Processing and characterization of a novel distributed strain sensor using carbon nanotube-based nonwoven composites. Sensors 15:17728–17747. https://doi.org/10.3390/s150717728
8. Zhai T, Li D, Fei G, Xia H (2015) Piezoresistive and compression resistance relaxation behavior of water blown carbon nanotube/polyurethane composite foam. Compos Part A 72:108–114. https://doi.org/10.1016/j.compositesa.2015.02.003
9. Moghaddam MK, Breede A, Brauner C, Lang W (2015) Embedding piezoresistive pressure sensors to obtain online pressure profiles inside fiber composite laminates. Sensors 15:7499–7511. https://doi.org/10.3390/s150407499
10. Yu X, Kwon E (2009) A carbon nanotube/cement composite with piezoresistive properties. Smart Mater Struct 18:055010. https://doi.org/10.1088/0964-1726/18/5/055010
11. Chung DDL (1998) Self-monitoring structural materials. Mater Sci Eng Rev 22:57–78. https://doi.org/10.1016/S0927-796X(97)00021-1
12. Chung DDL (2004) Electrically conductive cement-based materials. Adv Cem Res 16:167–176. https://doi.org/10.1680/adcr.2004.16.4.167

13. Chung DDL (2012) Carbon materials for structural self-sensing, electromagnetic shielding and thermal interfacing. Carbon 50:3342–3353. https://doi.org/10.1016/j.carbon.2012.01.031
14. Sugiyama S, Takigawa M, Igarashi I (1983) Integrated piezoresistive pressure sensor with both voltage and frequency output. Sens Actuators 4:113–120. https://doi.org/10.1016/0250-6874(83)85015-X
15. Porter TL, Eastman MP, Pace DL, Bradley M (2001) Sensor based on piezoresistive microcantilever technology. Sens Actuators A Phys 88:47–51. https://doi.org/10.1016/S0924-4247(00)00498-2
16. Roy AL, Sarkar H, Dutta A, Bhattacharyya TK (2014) A high precision SOI MEMS–CMOS piezoresistive accelerometer. Sens Actuators A Phys 210:77–85. https://doi.org/10.1016/j.sna.2014.01.036
17. Li X, Bao M, Yang H, Shen S, Lu D (1999) A micromachined piezoresistive angular rate sensor with a composite beam structure. Sens Actuators A Phys 72:217–223. https://doi.org/10.1016/S0924-4247(98)00220-9
18. Fragiacomo G, Ansbaek T, Pedersen T, Hansen O, Thomsen EV (2010) Analysis of small deflection touch mode behavior in capacitive pressure sensors. Sens Actuators A Phys 161:114–119. https://doi.org/10.1016/j.sna.2010.04.030
19. Wu X, Han Y, Zhang X, Lu C (2016) Highly sensitive, stretchable, and wash-durable strain sensor based on ultrathin conductive layer@ polyurethane yarn for tiny motion monitoring. ACS Appl Mater Interfaces 8:9936–9945. https://doi.org/10.1021/acsami.6b01174
20. Li F, Qi L, Yang J, Xu M, Luo X, Ma D (2000) Polyurethane/conducting carbon black composites: structure, electric conductivity, strain recovery behavior, and their relationships. J Appl Polym Sci 75:68–77. https://doi.org/10.1002/(SICI)1097-4628(20000103)75:1%3c68:AID-APP8%3e3.0.CO;2-I
21. Rodrigues PC, Akcelrud L (2003) Networks and blends of polyaniline and polyurethane: correlations between composition and thermal, dynamic mechanical and electrical properties. Polymer 44:6891–6899. https://doi.org/10.1016/j.polymer.2003.08.024
22. Chen SG, Hu XL, Hu J, Zhang MQ, Rong MZ, Zheng Q (2006) Relationships between organic vapor adsorption behaviors and gas sensitivity of carbon black filled waterborne polyurethane composites. Sens Actuators B 119:110–117. https://doi.org/10.1016/j.snb.2005.12.002
23. Zhao B, Fu RW, Zhang MQ, Zhang B, Zeng W, Rong MZ, Zheng Q (2007) Analysis of gas sensing behaviors of carbon black/waterborne polyurethane composites in low concentration organic vapors. J Mater Sci 42:4575–4580. https://doi.org/10.1007/s10853-006-0517-6
24. Bunde A, Dieterich W (2000) Percolation in composites. J Electroceram 5:81–92. https://doi.org/10.1023/A:1009997800513
25. Zheng S, Deng J, Yang L, Ren D, Huang S, Yang W, Liu Z, Mingbo Yang M (2014) Investigation on the piezoresistive behavior of high-density polyethylene/carbon black films in the elastic and plastic regimes. Compos Sci Technol 97:34–40. https://doi.org/10.1016/j.compscitech.2014.04.001
26. Strümpler R, Glatz-Reichenbach J (1999) Conducting polymer composites. J Electroceram 3:329–346. https://doi.org/10.1023/a:1009909812823
27. Sanches AO, Kanda DHF, Malmonge LF, Silva MJ, Sakamoto WK, Malmonge JA (2017) Synergistic effects on polyurethane/lead zirconate titanate/carbon black three-phase composites. Polym Test 60:253–259. https://doi.org/10.1016/j.polymertesting.2017.03.031
28. Guo X, Huang Y, Zhao Y, Mao L, Gao L, Pan W, Zhang Y, Liu P (2017) Highly stretchable strain sensor based on SWCNTs/CB synergistic conductive network for wearable human-activity monitoring and recognition. Smart Mater Struct 26:095017. https://doi.org/10.1088/1361-665X/aa79c3
29. Vionnet-Menot S, Grimaldi C, Maeder T, Strässler S, Ryser P (2005) Tunneling-percolation origin of nonuniversality: theory and experiments. Phys Rev B 71:064201. https://doi.org/10.1103/PhysRevB.71.064201
30. Flandin L, Hiltner A, Baer E (2001) Interrelationships between electrical and mechanical properties of a carbon black-filled ethylene–octene elastomer. Polymer 42:827–838. https://doi.org/10.1016/S0032-3861(00)00324-4
31. Luheng W, Tianhuai D, Peng W (2009) Influence of carbon black concentration on piezoresistivity for carbon-black-filled silicone rubber composite. Carbon 47:3151–3157. https://doi.org/10.1016/j.carbon.2009.06.050
32. Rebeque PV, Silva MJ, Cena CR, Nagashima HN, Malmonge JA, Kanda DHF (2019) Analysis of the electrical conduction in percolative nanocomposites based on castor-oil polyurethane with carbon black and activated carbon nanopowder. Polym Compos 40:7–15. https://doi.org/10.1002/pc.24588

33. Zhai T, Li D, Fei G, Xia H (2015) Piezoresistive and compression resistance relaxation behavior of water blown carbon nanotube/polyurethane composite foam. Compos Part A Appl Sci Manuf 72:108–114. https://doi.org/10.1016/j.compositesa.2015.02.003
34. Sobha AP, Narayanankutty SK (2015) Improved strain sensing property of functionalised multi-walled carbon nanotube/polyaniline composites in TPU matrix. Sens Actuators A 233:98–107. https://doi.org/10.1016/j.sna.2015.06.012
35. Mather PJ, Thomas KM (1997) Carbon black/high density polyethylene conducting composite materials: part II The relationship between the positive temperature coefficient and the volume resistivity. J Mater Sci 32:1711–1715. https://doi.org/10.1023/A:1018567731526
36. Petrović ZS, Martinović B, Divjaković V, Budinski-Simendić J (1993) Polypropylene–carbon black interaction in conductive composites. J Appl Polym Sci 49:1659–1669. https://doi.org/10.1002/app.1993.070490919
37. Fu SY, Feng XQ, Lauke B, Mai YW (2008) Effects of particle size, particle/matrix interface adhesion and particle loading on mechanical properties of particulate–polymer composites. Compos Part B Eng 39:933–961. https://doi.org/10.1016/j.compositesb.2008.01.002
38. Zhang S, Liu H, Yang S, Shi X, Zhang D, Shan C, Guo Z (2019) Ultrasensitive and highly compressible piezoresistive sensor based on polyurethane sponge coated with cracked cellulose nanofibril/silver nanowire layer. ACS Appl Mater Interfaces. https://doi.org/10.1021/acsami.9b00900
39. Christ JF, Hohimer CJ, Aliheidari N, Ameli A, Mo C, Pötschke P (2017) 3D printing of highly elastic strain sensors using polyurethane/multiwall carbon nanotube composites. Proc SPIE 10168:101680E. https://doi.org/10.1117/12.2259820
40. Das NC, Chaki TK, Khastgir D (2002) Effect of axial stretching on electrical resistivity of short carbon fibre and carbon black filled conductive rubber composites. Polym Int 51:156–163. https://doi.org/10.1002/pi.811
41. Aneli JN, Zaikov GE, Khananashvili LM (1999) Effects of mechanical deformations on the structurization and electric conductivity of electric conducting polymer composites. J Appl Polym Sci 74:601–621. https://doi.org/10.1002/(SICI)1097-4628(19991017)74:3%3c601:AID-APP14%3e3.0.CO;2-K
42. Yamaguchi K, Busfield JJC, Thomas AG (2003) Electrical and mechanical behavior of filled elastomers. J Polym Sci Part B Polym Phys 41:2079–2089. https://doi.org/10.1002/polb.10571
43. Busfield JJC, Thomas AG, Yamaguchi K (2005) Electrical and mechanical behavior of filled rubber. III. Dynamic loading and the rate of recovery. J Polym Sci Part B Polym Phys 43:1649–1661. https://doi.org/10.1002/polb.20452
44. Flandin L, Chang A, Nazarenko S, Hiltner A, Baer E (2000) Effect of strain on the properties of an ethylene–octene elastomer with conductive carbon fillers. J Appl Polym Sci 76:894–905. https://doi.org/10.1002/(SICI)1097-4628(20000509)76:6%3c894:AID-APP16%3e3.0.CO;2-K
45. Zhang R, Deng H, Valenca R, Jin J, Fu Q, Bilotti E, Peijs T (2013) Strain sensing behavior of elastomeric composite films containing carbon nanotubes under cyclic loading. Compos Sci Technol 74:1–5. https://doi.org/10.1016/j.compscitech.2012.09.016
46. Lillemose M, Spieser M, Christiansen NO, Christensen A, Boisen A (2008) Intrinsically conductive polymer thin film piezoresistors. Microelectron Eng 85:969–971. https://doi.org/10.1016/j.mee.2007.12.020
47. Ku-Herrera JJ, Avilés F, Seidel GD (2013) Self-sensing of elastic strain, matrix yielding and plasticity in multiwall/carbon nanotube vinyl ester composites. Smart Mater Struct 22:085003. https://doi.org/10.1088/0964-1726/22/8/085003
48. Zhou L, Jung S, Brandon E, Jackson TN (2006) Flexible substrate microcrystalline silicon and gated amorphous silicon strain sensors. IEEE Trans Electron Devices 53:380–385. https://doi.org/10.1109/TED.2005.861727
49. Stassi S, Cauda V, Canavese G, Pirri CF (2014) Flexible tactile sensing based on piezoresistive composites: a review. Sensors 14:5296–5332. https://doi.org/10.3390/s140305296
50. Theodosiou TC, Saravanos DA (2010) Numerical investigation of mechanisms affecting the piezoresistive properties of CNT doped polymers using multi-scale models. Compos Sci Technol 70:1312–1320. https://doi.org/10.1016/j.compscitech.2010.04.003
51. Hu N, Karube Y, Arai M, Watanabe T, Yan C, Li Y, Liu Y, Fukunaga H (2010) Investigation on sensitivity of a polymer/carbon nanotube composite strain sensor. Carbon 48:680–687. https://doi.org/10.1016/j.carbon.2009.10.012

52. Pham GT, Park YB, Liang Z, Zhang C, Wang B (2008) Processing and modeling of conductive thermoplastic/carbon nanotubes films for strain sensing. Compos Part B Eng 39:209–216. https://doi.org/10.1016/j.compositesb.2007.02.024
53. Bautista-Quijano JR, Avilés F, Aguilar JO, Tapia A (2010) A strain sensing capabilities of a piezoresistive MWCNT–polysulfone film. Sens Actuators A Phys 159:135–140. https://doi.org/10.1016/j.sna.2010.03.005
54. Zhang W, Suhr J, Koratkar N (2006) Carbon nanotube/polycarbonate composites as multifunctional strain sensors. J Nanosci Nanotechnol 6:960–964. https://doi.org/10.1166/jnn.2006.171
55. Yi W, Wang Y, Wang G, Tao X (2012) Investigation of carbon black/silicone elastomer/dimethyl-silicone oil composites for flexible strain sensors. Polym Test 31:677–684. https://doi.org/10.1016/j.polymertesting.2012.03.006
56. Oliva-Avilés AI, Avilés F, Sosa V (2009) Electrical and piezoresistive properties of multi-walled carbon nanotube/polymer composite films aligned by an electric field. Carbon 49:2989–2997. https://doi.org/10.1016/j.carbon.2011.03.017